

## Hall conductivity beyond the linear response regime

To cite this article: A. R. Kolovsky 2011 *EPL* **96** 50002

View the [article online](#) for updates and enhancements.

### Related content

- [Conductivity with cold atoms in optical lattices](#)  
A R Kolovsky
- [Landau-Stark states in finite lattices and edge-induced Bloch oscillations](#)  
Iliya Yu. Chesnokov and Andrey R. Kolovsky
- [Creating artificial magnetic fields for cold atoms by photon-assisted tunneling](#)  
A. R. Kolovsky

### Recent citations

- [System susceptibility and bound-states in structured reservoirs](#)  
H. Z. Shen *et al*
- [Linear response theory for periodically driven systems with non-Markovian effects](#)  
H. Z. Shen *et al*
- [Master equation for open two-band systems and its applications to Hall conductance](#)  
H Z Shen *et al*



**IOP | ebooks™**

Bringing together innovative digital publishing with leading authors from the global scientific community.

Start exploring the collection—download the first chapter of every title for free.

# Hall conductivity beyond the linear response regime

A. R. KOLOVSKY<sup>(a)</sup>

*Kirensky Institute of Physics - 660036 Krasnoyarsk, Russia*  
*Siberian Federal University - 660041 Krasnoyarsk, Russia*

received 11 July 2011; accepted in final form 6 October 2011  
published online 15 November 2011

PACS 05.60.Gg – Quantum transport  
PACS 73.43.-f – Quantum Hall effects

**Abstract** – This paper introduces a semi-analytical method for calculating the Hall conductivity in the single-band approximation. The method goes beyond the linear response theory and thus, it formally imposes no limitation on the electric-field magnitude. It is shown that, when the Bloch frequency exceeds the cyclotron frequency, the Hall current decreases with increasing electric field. The obtained results can be directly applied to the cold Bose atoms in a 2D optical lattice, where the single-band approximation is well justified.

Copyright © EPLA, 2011

**Introduction.** – Since the early works by Ohm in the XIX century [1], and up to the seventies of the XX century, all studies of conductivity in solid crystals have considered the weak-field regime, where the electric field can be treated as a perturbation. This approach was actually justified, because for typical laboratory conditions the Bloch frequency, which is proportional to the electric field, is much smaller than the characteristic relaxation rate in a crystal. This situation changed in 1970, when Esaki and Tsu published their pioneering work [2] on the Ohm current in semiconductor superlattices. It was predicted that increasing the electric field the current would reach some maximum value and then decrease —this phenomenon is known nowadays as negative differential conductivity (see eq. (1) below). Besides semiconductor superlattices [3–5], negative differential conductivity has been also observed for cold neutral atoms in (quasi-) 1D optical lattices subjected to a static force [6]. A great advantage of the latter system over semiconductor superlattices is that full experimental control of relaxation processes can be achieved. Because of this control, with cold atoms one can study both Hamiltonian and dissipative dynamics of the carriers, *i.e.*, Bloch oscillations and Ohmic current.

In this work we generalize the Esaki-Tsu approach to the case of 2D superlattices in the so-called Hall configuration, which implies the presence of a magnetic field. Needless to say, in this case one has two field effects: one on the longitudinal Ohm current and the other one on the transverse Hall current. In the linear regime the problem of Hall conductivity in 2D superlattices has been intensively

studied both theoretically and experimentally with respect to quantum dot and antidot arrays: see, [7–10], to cite just a few of some hundreds relevant papers. In the present work we study theoretically the Hall conductivity in the nonlinear regime. As a model we consider the tight-binding Hamiltonian of a carrier in crossing electric and magnetic fields. We note that besides semiconductor systems this model can be also realized with cold atoms in optical lattices, subjected to artificial electric and magnetic fields [11–13].

**Esaki-Tsu dependence for Ohmic current.** – First we recall the reader few results on ordinary conductivity in the non-perturbative regime. To explain the negative differential conductivity in semiconductor superlattices Esaki and Tsu used a kind of semiclassical approach, which resulted in the following dependence for the Ohm current:

$$\frac{v}{v_0} = f(T) \frac{\omega_B/\gamma}{1 + (\omega_B/\gamma)^2}, \quad \omega_B = \frac{edF}{\hbar}. \quad (1)$$

In eq. (1)  $F$  is the electric field,  $d$  the lattice period,  $e$  the electron charge,  $\gamma$  the relaxation constant, and the pre-factor  $f(T)$  accounts for the temperature dependence of the current [ $f(0) = 1$ ]. A microscopic derivation of the Esaki-Tsu dependence (1) was given by Minot in 2004 [14]. In the cited paper this was obtained by solving the master equation for the carriers one-particle density matrix  $\hat{\rho}$ :

$$\frac{d\hat{\rho}}{dt} = -\frac{i}{\hbar}[\hat{H}, \hat{\rho}] - \gamma(\hat{\rho} - \hat{\rho}_0). \quad (2)$$

In this equation  $\hat{H}$  is the single-particle Hamiltonian of a carrier in a biased superlattice,  $\hat{H} = \hat{H}_0 + edF \sum_l |l\rangle l \langle l|$ ,

<sup>(a)</sup>E-mail: andrey.r.kolovsky@gmail.com

$\hat{H}_0 = -\frac{J}{2} \sum_l (|l+1\rangle\langle l| + \text{h.c.})$ , and  $\hat{\rho}_0$  is the equilibrium density matrix for  $F=0$ ,  $\hat{\rho}_0 \sim \exp(-\hat{H}_0/k_B T)$ . The model (2) results in eq. (1) with the correct temperature prefactor  $f(T)$ .

The above microscopic derivation of the Esaki-Tsu dependence was revisited in ref. [15] with respect to the problem of ordinary conductivity with cold atoms in 1D optical lattices. A weak point of the master equation (2) is that it is not in the Lindblad form. (Exclusions are the cases of zero and infinite temperature, where it can be rewritten in the Lindblad form.) Because of this drawback it may give incorrect result for the velocity distribution of the carriers [15]. However, it was confirmed that it gives qualitatively (and even semi-quantitatively) correct result for the mean velocity, *i.e.*, the current. The master equation (2) will be our theoretical framework in studying the Hall conductivity in 2D lattices.

**The model.** – Now we consider a quantum particle in a square 2D lattice. The particle is subjected to an in-plane electric field  $F$ , aligned with the  $y$ -axis, and a magnetic field  $B$  normal to the  $x$ - $y$  plane. Using the tight-binding approximation and the gauge  $\mathbf{A} = B(-y, 0, 0)$  the particle Hamiltonian reads

$$\hat{H} = \hat{H}_0 + edF \sum_{l,m} |l,m\rangle m \langle l,m|, \quad (3)$$

where

$$\begin{aligned} \hat{H}_0 = & -\frac{J_x}{2} \sum_{l,m} (|l+1,m\rangle\langle l,m| e^{i2\pi\alpha m} + \text{h.c.}) \\ & -\frac{J_y}{2} \sum_{l,m} (|l,m+1\rangle\langle l,m| + \text{h.c.}). \end{aligned} \quad (4)$$

The dimensionless parameter  $\alpha$  in (4) is the Peierls phase, which is given by number of magnetic flux quanta per unit-cell area,  $\alpha = eBd^2/\hbar c$ . Besides the Peierls phase  $\alpha$  and the Bloch frequency  $\omega_B = edF/\hbar$  the other important characteristics of the system are the carrier effective mass,  $M^* = d^2(J_x J_y)^{1/2}/\hbar^2$ , the cyclotron frequency,  $\omega_c = eB/cM^* = 2\pi\alpha(J_x J_y)^{1/2}/\hbar$ , and the drift velocity  $v^* = ceF/B = d^2eF/\hbar\alpha$ . We note that for a charged particle (electron in a solid crystal) the Hamiltonian (4) can be justified only in the limit of small  $\alpha$ , where the cyclotron radius of the classical orbit essentially exceeds the lattice period. This is, however, not the case for cold atoms in optical lattices, where the actual parameter of the system is the Peierls phase but not the magnitude of a magnetic field [11,12]. Hence, we impose no limitations on  $\alpha$  and, without any loss of generality, one may consider  $|\alpha| \leq 1/2$ .

Our aim is to calculate the Hall ( $v_x$ ) and the Ohm ( $v_y$ ) currents,

$$v_{x,y} = \text{Tr}[\hat{v}_{x,y} \hat{\rho}_{st}], \quad (5)$$

where  $\hat{\rho}_{st}$  is the stationary solution of the master equation (2) and  $\hat{v}_{x,y}$  the current operators:  $\hat{v}_x = -\frac{i}{\hbar} [\hat{H}_0, \hat{x}]$

with  $\hat{x} = d \sum_{l,m} |l,m\rangle l \langle l,m|$ , and for  $\hat{v}_y$  one has a similar expression. Substituting (4) in the last equation we have

$$\begin{aligned} \hat{v}_x = & \frac{v_0^{(x)}}{2i} \sum_{l,m} (|l+1,m\rangle\langle l,m| e^{i2\pi\alpha m} - \text{h.c.}), \\ \hat{v}_y = & \frac{v_0^{(y)}}{2i} \sum_{l,m} (|l,m+1\rangle\langle l,m| - \text{h.c.}), \end{aligned} \quad (6)$$

where  $v_0^{(x,y)} = dJ_{x,y}/\hbar$ .

**Landau-Stark states.** – We shall perform calculations in the basis of the Landau-Stark states, which are the eigenstates of the Hamiltonian (3). To simplify equations, we set the lattice period  $d$  and the Planck constant  $\hbar$  to unity from now on.

One finds the Landau-Stark states semi-analytically by using the following ansatz [16,17]:

$$|\Psi\rangle = \sum_{l,m} \frac{e^{i\kappa l}}{\sqrt{L_x}} b_m |l,m\rangle. \quad (7)$$

In eq. (7)  $\kappa = 2\pi k/L_x$  is the quasimomentum,  $0 \leq \kappa < 2\pi$ ,  $L_x$  the lattice size in the  $x$  direction and we eventually let  $L_x$  tend to infinity. Substituting (7) into the stationary Schrödinger equation with the Hamiltonian (3), we reduce it to the following 1D eigenvalue problem:

$$-\frac{J_y}{2} (b_{m+1} + b_{m-1}) + [Fm - J_x \cos(2\pi\alpha m - \kappa)] b_m = E b_m. \quad (8)$$

Equation (8) is a kind of the 1D Wannier-Stark problem and can be easily solved numerically. Labeling the solution by the discrete index  $\nu$  and scanning over the quasimomentum  $\kappa$  we find the energy spectrum  $E = E_\nu(\kappa)$  and the Landau-Stark states  $|\Psi_{\nu,\kappa}\rangle$ .

The energy spectrum and properties of the Landau-Stark states were studied in some detail in our recent work [18] devoted to Hamiltonian dynamics of the system (3). (Note that in ref. [18] we use different Landau gauge with the vector potential  $\mathbf{A} = B(0, x, 0)$ .) As an example, fig. 1 shows the energy spectrum for  $J_x = J_y = 1$ ,  $\alpha = 1/10$ , and two different values of  $F$ . This figure is aimed to illustrate a qualitative change in the spectrum, which takes place around

$$F_{cr} = 2\pi\alpha J_x. \quad (9)$$

Namely, for  $F < F_{cr}$  the energy bands form a pattern with straight lines. The Landau-Stark states belonging to these lines are the transporting states, which transport the quantum particle in orthogonal to the field direction with the drift velocity  $v^* = F/2\pi\alpha$  [18].

Having the Landau-Stark states obtained we calculate the current operators (6) in this basis. We have  $\langle \Psi_{\nu,\kappa} | \hat{v}_{x,y} | \Psi_{\nu',\kappa'} \rangle = v_0^{(x,y)} \delta(\kappa - \kappa') V_{\nu,\nu'}^{(x,y)}(\kappa)$ , where

$$V_{\nu,\nu'}^{(x)}(\kappa) = \sum_m b_m^{(\nu)}(\kappa) b_m^{(\nu')}(\kappa) \sin(2\pi\alpha m - \kappa) \quad (10)$$

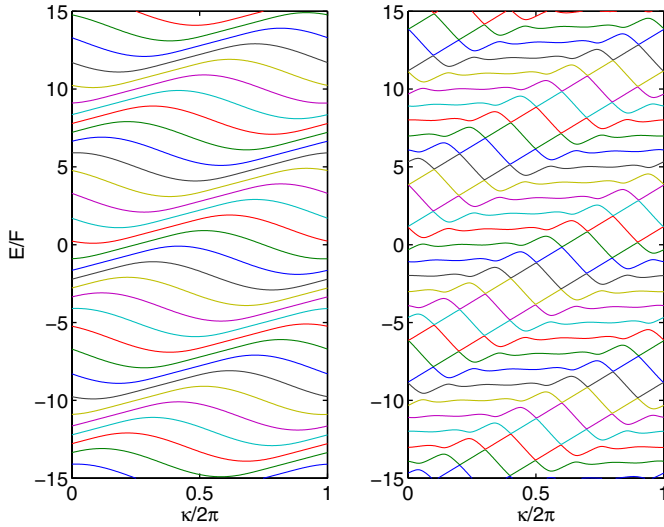


Fig. 1: (Colour on-line) A fragment of the energy spectrum of the Landau-Stark states for  $J_x = J_y = 1$ ,  $\alpha = 1/10$ , and  $F = 1$  (left) and  $F = 0.3$  (right).

and

$$V_{\nu,\nu'}^{(y)}(\kappa) = \sum_m \left[ b_{m+1}^{(\nu)}(\kappa) - b_{m-1}^{(\nu)}(\kappa) \right] b_m^{(\nu')}(\kappa). \quad (11)$$

Because of the presence of the  $\delta$ -function in matrix elements, eq. (5) for the mean currents simplifies to

$$v_{x,y} = \frac{1}{2\pi} \int_0^{2\pi} d\kappa \text{Tr}[V^{(x,y)}(\kappa) \mathcal{R}^{(st)}(\kappa)], \quad (12)$$

where  $\mathcal{R}_{\nu,\nu'}^{(st)}(\kappa) = \langle \Psi_{\nu,\kappa} | \hat{\rho}_{st} | \Psi_{\nu',\kappa} \rangle$  is the  $\kappa$ -specific stationary density matrix,

$$\mathcal{R}_{\nu,\nu'}^{(st)}(\kappa) = \frac{\gamma}{\gamma + i[E_{\nu'}(\kappa) - E_{\nu}(\kappa)]} \mathcal{R}_{\nu,\nu'}^{(0)}(\kappa). \quad (13)$$

**Landau states.** – Next we specify the equilibrium density matrix  $\hat{\rho}_0$ . To have tractable results we shall consider the case where only the lowest Landau level is populated. Thus we assume

$$\hat{\rho}_0 = \frac{1}{\mathcal{N}} \sum_{j=1}^{\mathcal{N}} |\Phi_j\rangle \langle \Phi_j|, \quad (14)$$

where  $\mathcal{N} = \alpha L_y L_x$  and  $|\Phi_j\rangle$  are the lowest energy Landau states. The density matrix (14) corresponds to  $\mathcal{N}$  fermionic carriers at zero temperature. Alternatively, it may be considered as a density matrix of non-interacting bosons at a finite temperature. We adopt the latter point of view, where the relevant temperature interval is discussed below. We would like to stress that our choice of the equilibrium density matrix is exclusively for the sake of easy interpretation of numerical results. In principle, one may consider an arbitrary  $\hat{\rho}_0$ . This way the reported results can be generalized to arbitrary temperature and arbitrary carrier statistics.

Similar to the case of Landau-Stark states, one finds the Landau states semi-analytically by setting  $F = 0$  in eq. (8), which reduces it to the Harper problem [19]. Figure 2 shows the integrated density of states of the Harper Hamiltonian for  $\alpha = 1/20$  and  $\alpha = 1/10$ . The states  $|\Phi_j\rangle$  in (14) are associated with the first step in the integrated density of the height  $\mathcal{N} = 80$  and  $\mathcal{N} = 160$ , respectively. It is also easy to show that the length of this step is approximately given by the cyclotron energy  $\hbar\omega_c = 2\pi\alpha(J_x J_y)^{1/2}$ . Thus our condition on the temperature reads  $k_B T \ll \hbar\omega_c$ . At the same time, to have equal populations of the lowest Landau states, we assume  $k_B T \gg \Delta$ , where  $\Delta$  is the width of the lowest magnetic band<sup>1</sup>.

**Numerical procedure and results.** – Our numerical procedure is as follows. We fix  $L_x$  and  $L_y$  and calculate the Landau and Landau-Stark states. The lattice size  $L_x$  defines a discrete step for the quasimomentum, which should be small enough to resolve main quasi-crossings in fig. 1. The lattice size  $L_y$  is arbitrary yet, to reduce the boundary effect when solving (8),  $L_y \gg 1/\alpha$ . Next we calculate the  $\kappa$ -specific matrices of the current operators and the stationary density matrix (13). We note in passing that for a rational  $\alpha = r/q$  infinite matrices of the current operators and the  $\kappa$ -specific density matrix obey the translational symmetry,

$$V_{\nu'+q,\nu+q}^{(x,y)}(\kappa) = V_{\nu',\nu}^{(x,y)}(\kappa), \quad \mathcal{R}_{\nu'+q,\nu+q}^{(st)}(\kappa) = \mathcal{R}_{\nu',\nu}^{(st)}(\kappa), \quad (15)$$

which further facilitates the numerical procedure. Finally, substituting these matrices into (12) and integrating over the quasimomentum  $\kappa$  we calculate the Hall and Ohm currents.

The left panel in fig. 3 shows the Hall current  $v_x$  as a function of the applied field  $F$  for  $\alpha = 1/10$  and different values of the relaxation constant  $\gamma$ . We begin with considering the case  $\gamma = 0$  (thin solid line), which corresponds to Hamiltonian dynamics of the carriers. As shown in ref. [18], for the specified initial conditions (population of the ground Landau level) a weak static field transports the carriers in the orthogonal direction with the drift velocity. Thus in the weak-field regime the dependence  $v_x = v_x(F)$  is approximated by  $v_x = F/2\pi\alpha$ . An increase in the Hall current continues till  $F$  reaches some critical value  $F^*$ , where the function  $v_x = v_x(F)$  has a global maximum. An estimate for  $F^*$  is provided by eq. (9), although we found  $F^*$  to be systematically larger than  $F_{cr}$  by a numerical factor  $1 < z < 2$  (see fig. 4 (left)). With further growth of the electric field we enter the regime of negative differential conductivity, where the Hall current decreases with the increase of  $F$ .

<sup>1</sup>Here we use the notion of the magnetic band irrespectively of the commensurability condition. In the other words,  $\Delta$  is the width of the vertical part of a step in the integrated density of state, which is essentially the same for a rational  $\alpha$  and irrational  $\alpha' \approx \alpha$ .

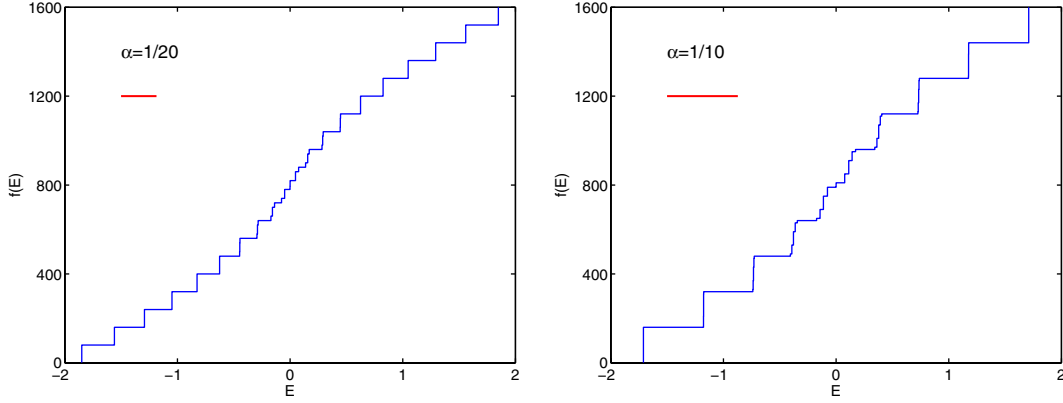


Fig. 2: (Colour on-line) Integrated density of states of the system (4) for  $\alpha=1/20$  (left) and  $\alpha=1/10$  (right). The other parameters are  $J_x = J_y = 1$  and  $L_x = L_y = 40$ . A piece of straight line indicates the energy interval  $\hbar\omega_c$ .

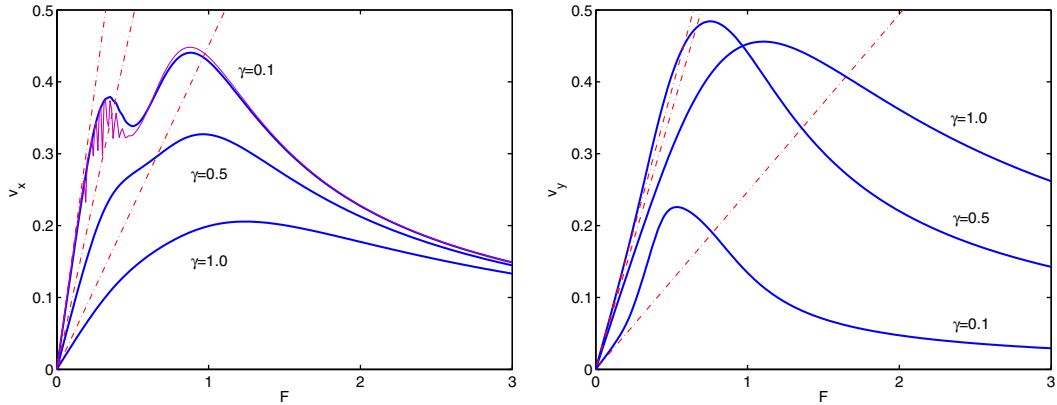


Fig. 3: (Colour on-line) The Hall (left) and Ohm (right) currents as functions of the electric field  $F$  for  $\alpha=1/10$  and different relaxation rates  $\gamma$ . The straight dash-dotted lines are predictions of the linear response theory. Additional thin solid line in the left panel shows the Hall current for  $\gamma=0$ , where the Ohm current vanishes.

As mentioned above, one finds an explanation for the transition from positive to negative differential conductivity regimes in structural changes of the Landau-Stark states, which take place around  $F_{cr}$ . Another explanation is based on the Landau states picture. Namely, using the Kramers-Hennenberger transformation an electric field is seen as periodic driving of the system with the Bloch frequency  $\omega_B = F$ . When  $\omega_B$  matches the energy gap between the ground and the first magnetic band (*i.e.*, the length of the first step in fig. 2, approximately given by the cyclotron frequency  $\omega_c$ ), the driving induces transitions between the Landau levels and we observe the local minimum in the dependence  $v_x = v_x(F)$ , which always precedes the global maximum.

The other (solid) lines in fig. 3 (left) show the dissipative Hall current for  $\gamma=0.1, 0.5, 1$ . It is seen that a finite relaxation rate suppresses the Hall current and smoothes the fine features of the dependence  $v_x = v_x(F)$  for the non-dissipative Hall current. In addition to fig. 3 (left) the left panel in fig. 4 shows the Hall current for fixed  $\gamma=0.1$  and different  $\alpha$ . The vertical dashed lines in this figure indicate the critical electric field (9) for each case.

The right panels in fig. 3 and fig. 4 show the Ohm current. It is seen in fig. 3 that larger relaxation rates suppress the Hall current but enhance the Ohm current. In the limit  $\gamma \rightarrow \infty$  the Hall current vanishes and the dependence  $v_y = v_y(F)$  for the Ohm current approaches the Esaki-Tsu dependence (1). Alternatively, one recovers the Esaki-Tsu result by considering the limit  $\alpha \rightarrow 0$ , see fig. 4 (right). In fig. 3 and fig. 4 we also depict predictions of the linear response theory,  $\mathbf{v} = \sigma \mathbf{F}$ , where the off-diagonal and diagonal elements of the conductivity tensor are given by the Drude-type formulas

$$\sigma_{xy} = \frac{1}{\gamma} \frac{\omega_c/\gamma}{1 + (\omega_c/\gamma)^2}, \quad \sigma_{yy} = \frac{1}{\gamma} \frac{1}{1 + (\omega_c/\gamma)^2}. \quad (16)$$

**Conclusions.** – We considered the quantum particle in a 2D lattice subject to (real or artificial) electric and magnetic fields and calculated the Hall and Ohm currents as functions of the electric-field magnitude. Although the obtained dependence  $v_x = v_x(F)$  for the Hall current resembles the Esaki-Tsu dependence  $v_y = v_y(F)$  for the Ohm current in the absence of magnetic field, the physics behind these two dependences is completely different.



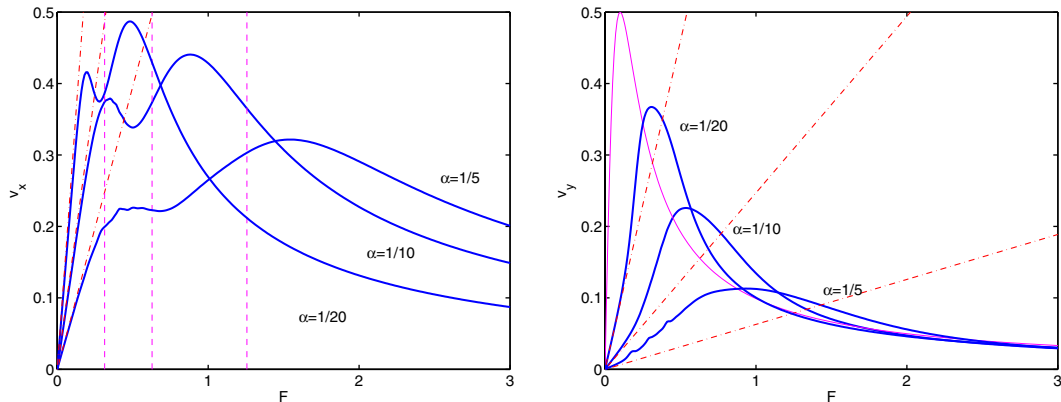


Fig. 4: (Colour on-line) The Hall (left) and Ohm (right) currents as functions of electric field  $F$  for  $\gamma = 0.1$  and different  $\alpha$ . Additional thin solid line in the right panel shows the Ohm current for  $\alpha = 0$ , where the Hall current vanishes.

Indeed, the Esaki-Tsu dependence for the Ohm current appears due to an interplay between Bloch oscillations and relaxation processes and the Ohm current vanishes if  $\gamma = 0$ . Conversely, the Hall current in the transverse direction takes place even in the absence of dissipation. The actual reason for the Esaki-Tsu-like dependence for the Hall current is a qualitative change in the structure of the Landau-Stark states, which happens around  $F_{cr}$ . Note that the condition  $F = F_{cr}$  means that the Bloch frequency coincides with the cyclotron frequency. Thus the Esaki-Tsu-like dependence for the Hall current is the result of an interplay between Bloch and cyclotron oscillations but not Bloch oscillations and relaxation processes.

Let us discuss possible candidates for a laboratory experiment, where the depicted dependences could be measured. As mentioned in the introductory section, it can be a semiconductor quantum dot (antidot) array. The main problem one encounters here is that the Fermi energy of electrons in a typical dot array lies outside the ground Bloch miniband and, hence, the single-band approximation (which is used throughout the paper) may be questioned. Beside this, in the semiconductor systems the relaxation processes are mainly due to electron-phonon interactions and, thus, the relaxation rate  $\gamma$  can be varied only in relatively narrow interval.

Cold neutral atoms in an 2D optical lattice looks a better candidate. Here the single-band approximation is perfectly justified as soon as the optical lattice is deeper than few recoil energies. Next, the dimensional static force  $F$  (*i.e.*, the Stark energy measured in units of the tunneling energy  $J$ ) can be set to very large values by simply increasing the lattice depth. For example, for cesium atoms in the gravitational field we have  $5.8 < F < 33.1$  for the lattice depth between 3 and 20 recoil energies. In addition, the region of small  $F$  is reached by using the magnetic levitation [20] to compensate, partially or completely, the gravitational field. However, the main advantage of the cold atoms system is a possibility to vary the relaxation rate. This was demonstrated in the experiment [6], which studies oscillations of spin polarized Fermi atoms in a

quasi-1D parabolic lattice in the presence of a buffer gas of Bose atoms. Theoretical analysis of this setup [21,22] results in the following expression for the relaxation rate,  $\Gamma \approx 3n^2U^2/\hbar J$ , where  $U$  is the on-site microscopic interaction constant (proportional to the  $s$ -wave scattering length of collisions between Bose and Fermi atoms) and  $n$  the density of the buffer gas (the mean occupation number of a lattice site). It follows from the displayed equation that the relaxation rate can be adjusted to a desired value either by varying the density of the buffer gas or by changing the  $s$ -wave scattering length for example, by means of the Feshbach resonance. Assuming  $n \sim 1$  and  $U \sim J$ , we obtain a dimensionless relaxation constant  $\gamma = \hbar\Gamma/J$  of the order of unity. Thus the dimensionless numerical parameters used above perfectly fit the actual physical parameters of the system.

Concluding the discussion we would like to stress that in this work we do not address the quantum Hall effect. The latter phenomenon occurs for fermionic carriers when the magnetic field or the Fermi energy are varied. It would be interesting to study the quantum Hall effect in the non-perturbative regime, where the conductivity tensor depends on the electric-field magnitude<sup>2</sup>. This problem is reserved for future studies.

\*\*\*

This work was supported by Russian Foundation for Basic Research, grant RFBR-10-02-00171-a.

## REFERENCES

- [1] OHM G. S., *Die galvanische Kette: mathematisch bearbeitet* (Riemann, Berlin) 1827.
- [2] ESAKI L. and TSU R., *IBM J. Res. Dev.*, **14** (1970) 61.

<sup>2</sup>With respect to quantum dots array this problem was addressed earlier in ref. [23,24]. However, these papers analyze a different model, where the starting point is Landau levels for free electron gas with the electron mass substituted by the effective mass.

- [3] SIBILLE A., PALMIER J. F., MINOT C. and MOLLOT F., *Appl. Phys. Lett.*, **54** (1989) 165.
- [4] SIBILLE A., PALMIER J. F., WANG H. and MOLLOT F., *Phys. Rev. Lett.*, **64** (1990) 52.
- [5] RAUCH C., STRASSER G., UNTERRAINER K., BOXLEITNER W., GORNIK E. and WACKER A., *Phys. Rev. Lett.*, **81** (1998) 3495.
- [6] OTT H., DE MIRANDES E., FERLAINO F., ROATI G., MODUGNO G. and INGUSCIO M., *Phys. Rev. Lett.*, **92** (2004) 160601.
- [7] GERHARDS R. R., WEISS D. and VON KLITZING K., *Phys. Rev. Lett.*, **62** (1989) 1173.
- [8] FLEISCHMANN R., GEISEL T. and KETZMERICK R., *Phys. Rev. Lett.*, **68** (1992) 1367.
- [9] WEISS D., RICHTER K., VASILIOU E. and LIITJERING G., *Surf. Sci.*, **305** (1994) 408.
- [10] ISHIZAKA S., NIHEY F., NAKAMURA K. and SONE J., *Phys. Rev. B*, **51** (1995) 9881.
- [11] JAKSCH D. and ZOLLER P., *New J. Phys.*, **5** (2003) 56.
- [12] KOLOVSKY A. R., *EPL*, **93** (2011) 20003.
- [13] LIN Y.-J., COMPTON R. L., JIMÉNEZ-GARCÍA K., PORTO J. V. and SPIELMAN I. B., *Nature*, **462** (2009) 628.
- [14] MINOT C., *Phys. Rev. B*, **70** (2004) 161309.
- [15] KOLOVSKY A. R., *Phys. Rev. A*, **77** (2008) 063604.
- [16] NAKANISHI T., OHTSUKI T. and SAITOH M., *J. Phys. Soc. Jpn.*, **64** (1995) 2092.
- [17] MUÑOZ E., BARTICEVIC Z. and PACHECO M., *Phys. Rev. B*, **71** (2005) 165301.
- [18] KOLOVSKY A. R. and MANTICA G., *Phys. Rev. E*, **83** (2011) 041123.
- [19] HOFSTADTER D. R., *Phys. Rev. B*, **14** (1976) 2239.
- [20] HALLER E., HART R., MARK M. J., DANZL J. G., REICHSÖLLNER L. and NÄGERL H.-CH., *Phys. Rev. Lett.*, **104** (2010) 200403.
- [21] PONOMAREV A. V., MANDROÑERO J., KOLOVSKY A. R. and BUCHLEITNER A., *Phys. Rev. Lett.*, **96** (2006) 050404.
- [22] KOLOVSKY A. R., *J. Stat. Mech.* (2009) P02018.
- [23] KUNOLD A. and TORRES M., *Quantum Hall effect beyond the linear response approximation*, arXiv:cond-mat/0311111 (2003).
- [24] KUNOLD A. and TORRES M., *Phys. Rev. B*, **80** (2009) 205314.